Journal of Sustainable Construction Materials and Technologies
Web page info: https://jscmt.yildiz.edu.tr
DOI: 10.47481/jscmt.1383493

JSCMT

Journal of Sustainable Construction
Materials and Technologies

Research Article

Effect of mineral admixtures and curing regimes on properties of self-compacting concrete

Chava VENKATESH*[iD], **M. V. Seshagiri RAO**[iD], **Munugala PRAVEEN KUMAR**[iD],
Chereddy SONALI SRI DURGA[iD]

Department of Civil Engineering, CVR College of Engineering, Vastunagar, Mangalpalli, Ibrahimpatnam,
Ranga Reddy, Telangana, India

ARTICLE INFO

ABSTRACT

This study investigated the influence of mineral admixtures (fly ash, silica fume, metakaolin) and curing conditions (water immersion, polyethylene glycol, gunny bags, accelerated curing) on the properties of self-compacting concrete (SCC). The rheological properties, compressive strength, chloride penetration resistance, and microstructure were evaluated. Incorporating mineral admixtures improved the workability, strength (up to 53% increase), and durability of SCC compared to plain mixes, with 20% metakaolin replacement optimal. Water immersion curing enhanced the compressive strength (3–15% increase) and chloride resistance (up to 30% decrease in migration coefficient) owing to improved hydration and microstructural refinement. Mineral admixtures reduced the sensitivity of SCC to the curing method. Microstructural analysis showed higher density and additional C-S-H phases with mineral admixtures under wet curing. The study demonstrates that optimized SCC containing appropriate supplementary cementitious materials and proper external curing can achieve high performance.

Cite this article as: Venkatesh, C., Rao. M. V. S., Kumar, M. P., & Sonali Sri Durga, C. (2024). Effect of mineral admixtures and curing regimes on properties of self-compacting concrete. *J Sustain Const Mater Technol*, 9(1), 25–35.

1. INTRODUCTION

Self-compacting concrete (SCC) represents a significant advancement in concrete technology that has revolutionized the construction industry over the past two decades. SCC is characterized by its ability to flow and compact under its weight without requiring external vibration, even in densely reinforced structural elements [1, 2]. Compared to conventional vibrated concrete, SCC offers several benefits, such as faster construction, reduced noise and labor, excellent surface finishes, and improved durability [3]. Eliminating vibration also enables the fabrication of complex architectural forms and intricate structural shapes that were previously not feasible [4].

The unique properties of SCC are achieved by careful mix design optimization to obtain the necessary rheological performance in the fresh state. This involves using chemical admixtures like superplasticizers coupled with proportioning powders, aggregates, water, and air content to achieve adequate flowability, passing ability, and resistance to segregation [5, 6]. However, SCC has some challenges, too. The high powder content needed to achieve robust self-compacting characteristics increases material costs. The reduction in coarse aggregate content also tends to lower the modulus of elasticity and creep resistance compared to traditional concrete [7]. Concerns about inadequate consolidation in highly congested members must be addressed through proper mix design and quality control [8].

A popular approach to addressing the challenges of SCC has been the incorporation of mineral admixtures as partial replacements for cement. Materials like fly ash, silica fume, ground granulated blast furnace slag, metakaolin, and rice husk ash, among others, have been investigated as cementitious components of SCC [9–11]. Compared to single or binary binder systems, ternary and quaternary blends utilizing mineral admixtures have shown improved rheology and stability owing to their particle size distribution benefits while enhancing technical properties like strength and durability due to their pozzolanic reactivity [12, 13].

Fly ash has been one of the most commonly studied mineral admixtures for SCC due to its spherical shape, satisfactory size, and pozzolanic nature [14]. Replacement levels of 15–35% have shown good performance, with flowability, segregation resistance, and compressive strength improved compared to plain Portland cement mixes [15]. Silica fume has been utilized at 5–10% dosages to enhance particle packing density, cohesiveness, and later-age strength development in SCC. However, higher additions can impair workability [16]. Ground granulated blast furnace slag has demonstrated the ability to maintain good rheology at replacement levels up to 50–60% while enhancing strength and durability via its latent hydraulic behavior [17].

Metakaolin has emerged as an increasingly popular pozzolanic additive for high-performance and architectural concretes. Its ultrafine particle size, high purity, and pozzolanic reactivity make it attractive as a SCC ingredient. Metakaolin has been shown to improve the stability, strength, and transport properties of SCC at replacement levels of 10–20% [18, 19]. Multi-blend SCC incorporating fly ash, slag, limestone, and metakaolin has also offered advantages over single or binary systems [20]. Rice husk ash, an agro-industrial byproduct, has demonstrated promising results as a supplementary cementing material in SCC, along with metakaolin and other mineral admixtures [21]. While significant research exists on the influence of different mineral admixtures on various SCC properties, there is further scope to optimize multi-blends to develop high-performance self-compacting concrete [22].

In addition to suitable materials selection through optimal mix design, proper curing is essential to achieve the performance potential of any concrete. Curing impacts the cement hydration reactions and governs the microstructural development, which controls the long-term properties related to strength and durability [23]. While SCC has shown superior performance when properly cured by water immersion, the need for practical and efficient curing that can be applied in field conditions has led to growing interest in alternative curing techniques. Accelerated curing using steam or heat can provide an early strength boost but may lead to delayed effects over time [24]. Membrane curing blocks moisture loss with limited effectiveness based on the barrier material [25]. Self-curing strategies using saturated lightweight aggregates, superabsorbent polymers, and chemical additives provide internal water reservoirs to sustain hydration [26].

Recent studies have investigated the influence of various external and internal curing techniques on the properties of conventional concrete and SCC [27–29]. Water im-

Table 1. Physical properties of aggregates

	Specific gravity	% of water absorption	Fineness modulus	Bulk density
Fine aggregates	2.69	1.10	2.56	1.46
Coarse aggregates	2.72	0.75	7.25	1.51

Table 2. Physical properties of SCMs

Properties	Cement	Fly ash	Silica fume	Metakaolin
Specific gravity	3.10	2.41	2.20	2.55
Specific surface area (m²/kg)	700	900	20000	11000
Color	Grey	Grey	Light grey	White
Average particle size (μm)	50	45	1	5

mersion is the optimal method, while polyethylene glycol showed promise as a self-curing agent for SCC [30]. However, limited studies compare different curing regimes for multi-blended SCC containing various mineral admixtures. There is also a need to correlate the curing effectiveness with the resultant microstructure of SCC using advanced characterization techniques. Therefore, this study aims to address some of the research gaps and make novel contributions by Systematically optimizing the design of high-performance self-compacting concrete utilizing multi-blends of fly ash, silica fume, and metakaolin as partial cement replacements and evaluating the influence of different practically relevant curing regimes, namely water immersion, membrane curing, accelerated curing, and self-curing on properties of the optimized SCC mixes and comparing the effectiveness of the various internal and external curing techniques based on the compressive strength as well as critical durability parameters like chloride migration coefficient and correlating the mechanical and durability performance to the resultant hydration and microstructure of SCC using sophisticated SEM-EDX analysis. The research outcomes are expected to guide the optimal selection of supplementary cementing materials and curing methods to develop durable and sustainable self-compacting concrete for advanced structural applications. The study will also generate predictive models relating curing conditions to SCC properties that can be applied for performance-based design and quality assurance.

2. MATERIALS AND METHODS

2.1. Materials

The study utilized ordinary Portland cement (OPC) of grade 53 as per ASTM C150 [31]. The physical and chemical properties confirm the codal provisions. IS used fine and coarse aggregates 383 – 2016 [32], and their physical properties are enlisted in Table 1. Figure 1 represents the size distribution of coarse and fine aggregates. The fly ash was obtained from local coal-based thermal industries, with a specific gravity of 2.41 and an average particle size of 45 μm, as shown in Table 2.
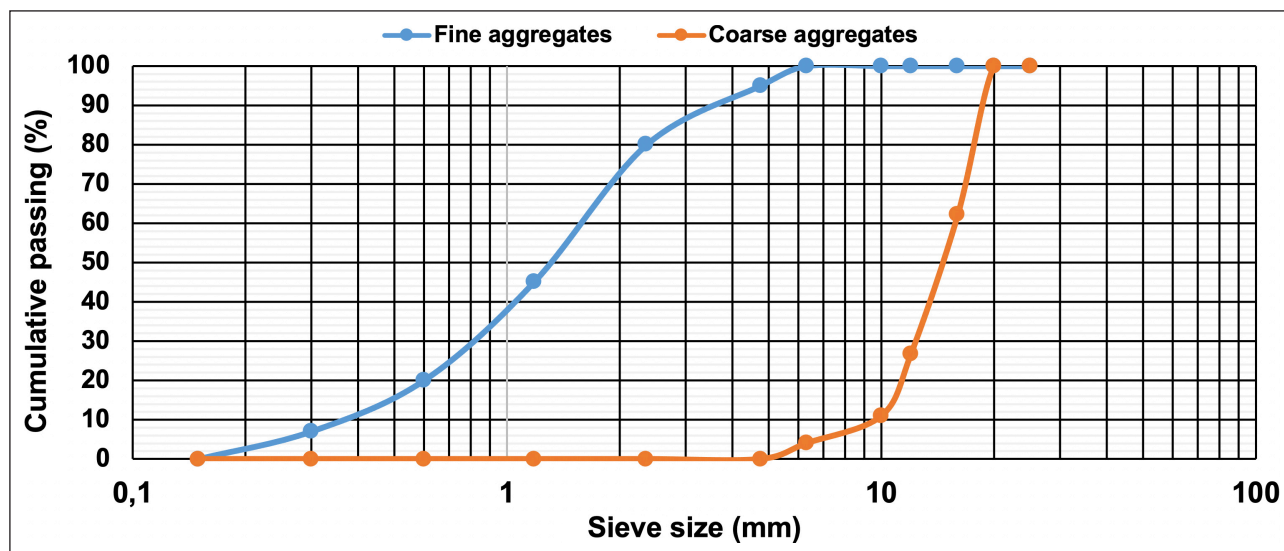
Figure 1. Aggregates size distribution.

Table 3. Chemical composition of binders (weight %)

Materials	CaO	SiO$_2$	Al$_2$O$_3$	Fe$_2$O$_3$	Na$_2$O	MgO	K$_2$O	TiO$_2$	Others
Cement	65.29	20.93	4.73	3.95	0.29	1.43	0.36	–	3.02
Fly ash	0.80	61	30.3	3.93	0.25	0.4	0.91	1.95	0.46
Silica fume	0.36	92	0.46	1.6	0.7	0.74	0.9	–	3.24
Metakaolin	0.1	52.1	36.1	4.3	–	0.84	1.38	–	5.18

Table 4. Physical properties of ROOF PLAST SP-455

Name of the chemical admixture	Appearance	Relative density (g/cm³)	pH	Compatible
ROOF PLAST SP-455	Brown colour	1.02–1.05	<6	For all sorts of cement

Table 5. Physical properties PEG-400

Name of the self-curing agent	Molecular weight	Appearance	Moisture	pH	Specific gravity
PEG-400	400	Clear Fluid	0.2%	6	1.2

Similarly, silica fume and metakaolin were procured from the local markets. Their specific gravities are 2.20 and 2.55, with average particle sizes of 1 μm and 5 μm, respectively. Table 3 shows the chemical composition of the binder (or mineral admixtures). The ROOFPLAST SP-455 was used as a water reducer in this study, and its properties are illustrated in Table 4. Polyethylene glycol-400 was used as a self-curing agent at a proportional level of 1% to the weight of the binder. Its specifications are listed in Table 5.

2.2. Mix Proportions

In the present study, 40MPa strength concrete was used for all the experiments, and its mix calculations were finalized according to the IS 10262-2019 [33], as shown in Table 6.

2.3. Rheological Studies

In the present study, all the rheological properties (namely, Flow test, V-Funnel, and L-Box) were evaluated according to the European Federation of National Associations Representing Concrete (EFNARC) guidelines [34].

2.3.1. L-box Test

Figure 2a represents the L-box; it is used to assess the passing ability of self-compacting concrete through tight openings like spaces between reinforcing bars. A vertical section and a horizontal area with a movable gate in between. Fill the vertical section and open the gate to let the concrete flow into the flat section. Measure the height of the concrete at the end of the flat section. Calculate the passing ability ratio as the height of concrete in the flat section divided by the height in the vertical section. A ratio of 0.8–1.0 indicates good passing ability.

2.3.2. V-funnel Test

Figure 2b depicts the V-funnel; it measures self-compacting concrete's flowability and filling ability. A V-shaped

Table 6. Mix proportions (Kg/m³)

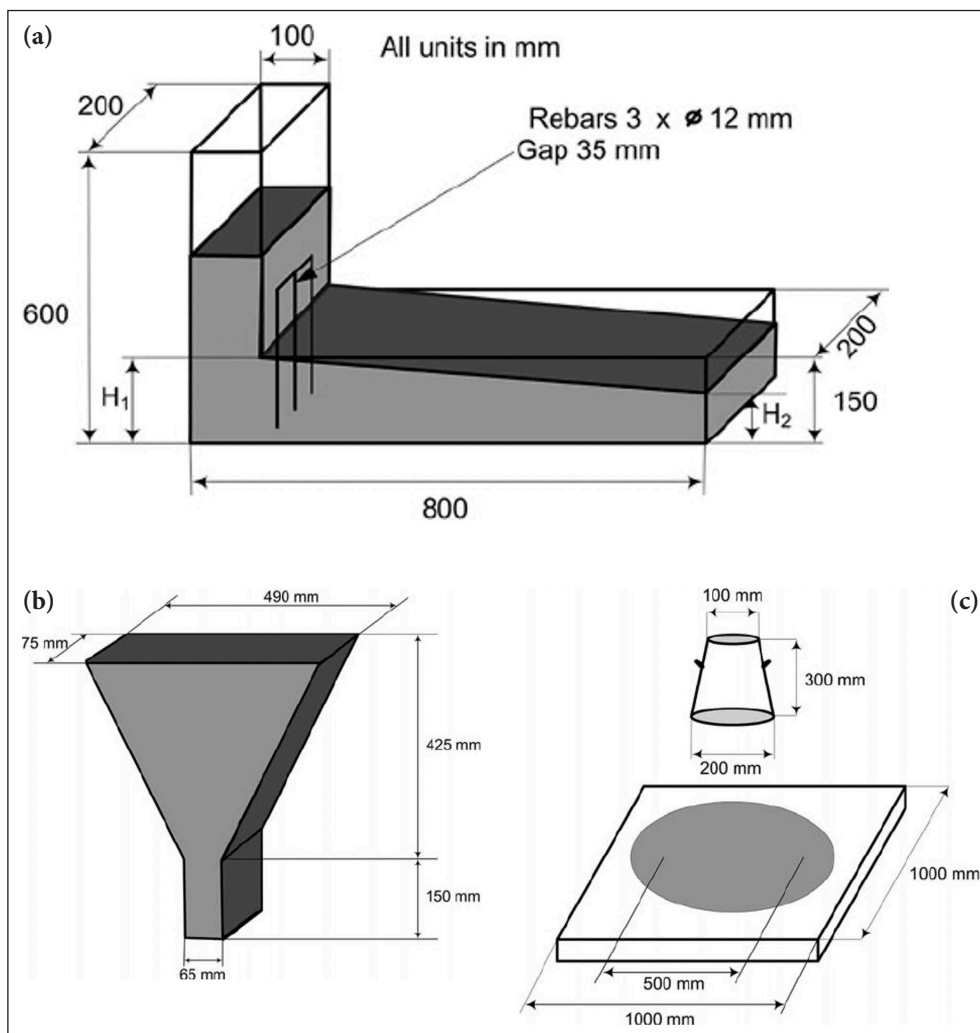| Mix no	Mix designation	OPC	FA	SF	MK	Fine aggregate	Coarse aggregate	SP (lit)	Water (lit)	w/b
M1	C100	531	–	–	–	891	786	9.34	185	0.35
M2	C60+FA40	319	212	–	–	891	786	9.34	185	0.35
M3	C85+MS15	452	–	79	–	891	786	9.34	185	0.35
M4	C80+MK20	425	–	–	106	891	786	9.34	185	0.35
M5	C35+MK15+FA50	186	265	–	73	891	786	9.34	185	0.35

Figure 2. **(a)** L-box. **(b)** V-funnel. **(c)** Slume cone and flow.

funnel with the bottom gate closed. Fill the funnel with concrete and open the gate. Measure the time the concrete takes to ultimately flow out of the funnel. Typical values are 6–12 seconds. Lower times indicate greater flowability.

2.3.3. T50 Slump Flow Test

Used to assess the horizontal free flow and filling ability of self-compacting concrete. Concrete is poured into a cone placed on a flat surface and lifted vertically. Measure the time the concrete takes to reach a diameter of 50 cm. Typical T50 times are 2–5 seconds. Lower times indicate better flowability. Figure 2c shows the slump cone.

2.3.4. Slump Flow Test

It has the same test procedure as the T50 slump flow. Instead of measuring T50 time, the final diameter of the concrete circle is measured. Diameters of 650–800mm indicate good flowability. Figure 2c represents the slump flow.

2.4. Curing Conditions

2.4.1. Water Immersion Curing

By ASTM C192-15 [35], water immersion curing involves fully submerging the hardened concrete component. This technique is commonly employed in laboratories for curing concrete

Figure 3. **(a)** Water immersion curing. **(b)** Self-curing with PEG-400. **(c)** Gunny bag membrane curing. **(d)** Accelerated curing.

specimens. It fulfills all curing requirements, including promoting hydration, reducing shrinkage, and dissipating heat during hydration. Water immersion curing is depicted in Figure 3a.

2.4.2. Accelerated Curing

Concrete is provided an early boost in compressive strength using the accelerated curing method. This study subjected the concrete mixes to accelerated curing conditions by ASTM C684-99 [36]. Under these conditions, the concrete will achieve full maturity within 28 hours. Figure 3b illustrates the experimental setup.

2.4.3. Membrane Curing

According to IRC-015 [37], gunny bag membrane curing was performed in the present study, and its experimental photograph is shown in Figure 3c.

2.4.4. Self-curing

In the present study, Polyethylene glycol-400 was employed as a self-curing agent in the self-compacting concrete, following the method outlined by Madduru et al. [38]. Experimental images are shown in Figure 3d.

Table 7. Rheological properties of different SCC mixes

Tests	EFNARC limits	M1	M2	M3	M4	M5
Flow test						
Slump (mm)	650–800	732	705	712	719	695
T-50 (Sec)	2–5	3.45	4.26	4.05	4.07	4.95
V-funnel	6–12	6.85	9.28	7.56	8.08	10.8
L-box	0.8–1	0.98	0.92	0.95	0.94	0.90

2.5. Compressive Strength

The value of uniaxial compressive stress achieved when a material completely fails is referred to as the material's compressive strength. Cube specimens measuring 150 mm x 150 mm x 150 mm were employed in this study and examined following IS 516: 1959 [39]. 60 cubic samples were prepared and cured under the above-selected curing conditions for up to 28 days.

2.6. Durability Properties

2.6.1. Rapid Chloride Permeability Test

They were used to measure the electrical conductance of concrete to provide a rapid indication of its resistance to the penetration of chloride ions. A 100 mm diameter, 50 mm thick concrete specimen is vacuum saturated and sealed between two cells containing calcium hydroxide solution. A 60V DC voltage is applied across the cell for 6 hours. The amount of electrical current passed through the specimen over this period is used to evaluate the resistance of concrete to chloride ion penetration. Charge passed is based on the current flow and time, according to the ASTM C1202 [40]. A lower coulomb value indicates higher resistance to chloride ion penetration.

2.6.2. Rapid Chloride Migration Test

They were used to determine the resistance of concrete to chloride ion penetration. A 50mm thick slice of 100mm diameter core is vacuum saturated. One face is exposed to a 2.8M NaCl solution. The other face to a 0.3M NaOH solution. A 30V DC voltage is applied for 24 hours. After testing, the specimen is split and sprayed with silver nitrate to measure chloride penetration depth, according to NT BUILD 492 [41]. The non-steady state migration coefficient is then calculated using the applied voltage, temperature, penetration depth, and test duration. A lower migration coefficient indicates higher resistance to chloride ion ingress.

2.7. Microstructural Properties

In the present study, the concrete sample's surface morphology and elemental composition were assessed using "Scanning Electron Microscope (SEM) and Energy Dispersive X-ray Spectroscopy analyses (EDX) [42–52]." The microstructure and elemental composition of the samples were analyzed using an SEM (Model: VEGA 3 Generation, TESCAN, Brno, Czech Republic) equipped with EDX spectroscopy (Model: EDAX-EDS-SSD, EDAX Inc., USA). Small pieces of the samples were mounted on aluminum stubs using carbon tape. A thin layer of gold was coated on the illustrations by sputter coating for 120 seconds at 10 mA (Model: 108 auto sputter coater, TED PELLA, INC.) to enhance the conductivity.

The surface morphology of gold-coated samples was examined under the SEM at an accelerating voltage of 10 kV and a working distance of 10–20 mm. Micrographs were taken at various magnifications ranging from 2.00kx to 5.00kx. For EDX analysis, the SEM was coupled with an EDX spectrometer. EDX spectra were collected at three spots on each sample to determine the elemental composition.

3. RESULTS AND DISCUSSION

3.1. Rheological Properties

The rheological properties of the various self-compacting concrete (SCC) mixes are presented in Table 7. All the mixes satisfied the EFNARC limits for slump flow, T50 slump flow, V-funnel, and L-box tests, indicating adequate flowability, filling, and passing ability. Mix M1 with 100% cement had the highest slump flow of 732 mm, while Mix M5 with 20% metakaolin replacement had the lowest slump of 695 mm. The reduced slump in M5 can be attributed to the higher water demand and increased viscosity caused by metakaolin's fine particle size and high pozzolanic reactivity.

3.2. Compressive Strength

The compressive strength results under different curing conditions are shown in Figure 4. The 28-day strengths ranged from 42.12 MPa for M1 under accelerated curing to 53.73 MPa for M5 under water immersion curing. All mixes showed increased strength with prolonged curing duration, as expected. Among the curing methods, water immersion consistently resulted in the highest compressive strengths, followed by polyethylene glycol, accelerated curing, and gunny bag curing. Water immersion provided a saturated environment that promoted better hydration and microstructural development than the other techniques. The strength gain under self-curing using polyethylene glycol was slightly lower, potentially due to some moisture loss over time. Accelerated steam curing generated higher early strength, but longer normal curing was needed to achieve later-age strengths similar to water immersion. Gunny bag curing was the least effective likely because it allowed greater moisture evaporation.

The relative compressive strength under different curing conditions compared to water immersion curing; Self-curing with polyethylene glycol achieved 92–96% of the strength under water curing. Accelerated curing re-
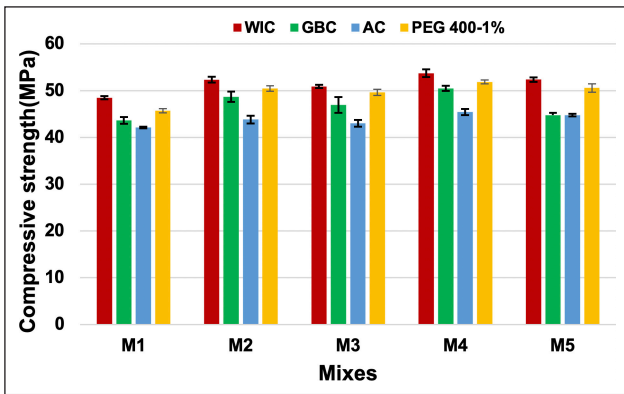
Figure 4. Compressive strength of concrete cured in various curing conditions.
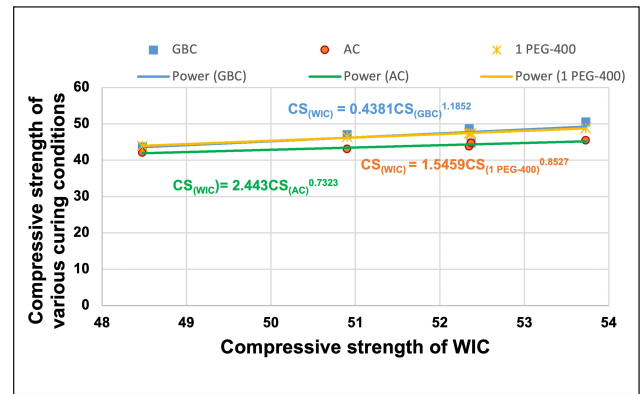

Figure 5. Relation between the compressive strength of WIC Vs other curing conditions.

Table 8. Chloride ions permeability and migration coefficient values

Mixes	Chloride ion migration coefficient ($\times 10^{-12}$ m²/s)							
	WIC		**GBC**		**AC**		**1 PEG-400**	
	Coefficient values	Standard deviation	Coefficient values	Standard deviation	Coefficient values	Standard deviation	Coefficient values	Standard deviation
M1	7.23	0.0436	9.2	0.2646	10.17	0.0300	8.45	0.0400
M2	4.86	0.0346	7.15	0.0300	7.66	0.0458	6.23	0.0265
M3	4.02	0.0608	5.13	0.0265	5.95	0.0265	4.27	0.0265
M4	3.42	0.0265	4.38	0.0200	5.5	0.0173	3.41	0.0173
M5	5.31	0.0200	6.89	0.0985	7.57	0.0300	5.87	0.0300

sulted in 87–93%, while gunny bag curing gave the lowest strengths of 78–85% of water-cured samples. This reinforces water immersion as the optimal curing technique. Among the mixes, the metakaolin blend M5 showed the smallest differences between curing methods, suggesting it was less sensitive to external curing. Its high reactivity and pozzolanic nature meant sufficient internal curing occurred through ongoing hydration reactions.

Figure 5 represents the relationship between the compressive strength during water immersion curing and other selected curing conditions. Through observation, a good correlation was found between the experimental results and the predicted values from the following equations: Eq. 1–Eq. 3.

i. Relation between WIC and GBC is as follows
$$CS_{(WIC)} = 0.4381 CS_{(GBC)}^{1.1852} \qquad \text{Eq.1}$$
ii. The relation between the WIC and AC is given below
$$CS_{(WIC)} = 2.443 CS_{(AC)}^{0.7323} \qquad \text{Eq.2}$$
iii. The relation between the WIC and 1 PEG-400 is given below
$$CS_{(WIC)} = 1.5459 CS_{(1\,PEG-400)}^{0.8527} \qquad \text{Eq.3}$$

3.3. Durability Studies

3.3.1. Rapid Chloride Migration Coefficient

The chloride ion migration coefficients in Table 8 indicate the resistance of the SCC mixes to chloride penetration. A lower migration coefficient represents lower permeabili-
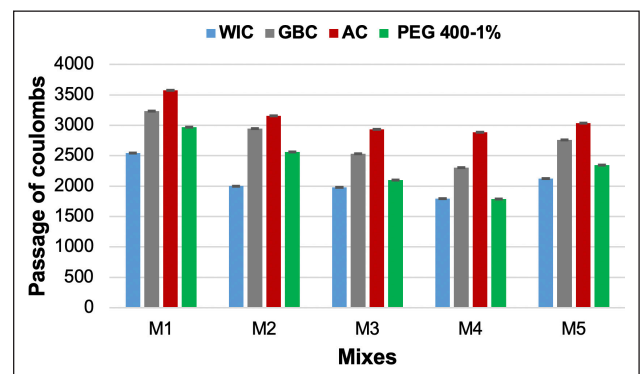

Figure 6. Rapid chloride permeability results.

ty. Incorporating mineral admixtures reduced the permeability notably compared to plain cement mix M1, with the metakaolin blend M5 showing the best performance. The excellent chloride resistance with supplementary cementitious materials can be attributed to pore refinement and reduced porosity from the pozzolanic reactions. Among curing techniques, water immersion curing again led to the lowest permeability, followed by polyethylene glycol, accelerated, and gunny bag curing. The denser microstructure with improved hydration under wet curing restricted chloride ingress. The permeability trends matched the compressive strength trends, suggesting the microstructural changes influencing strength also governed transport properties.
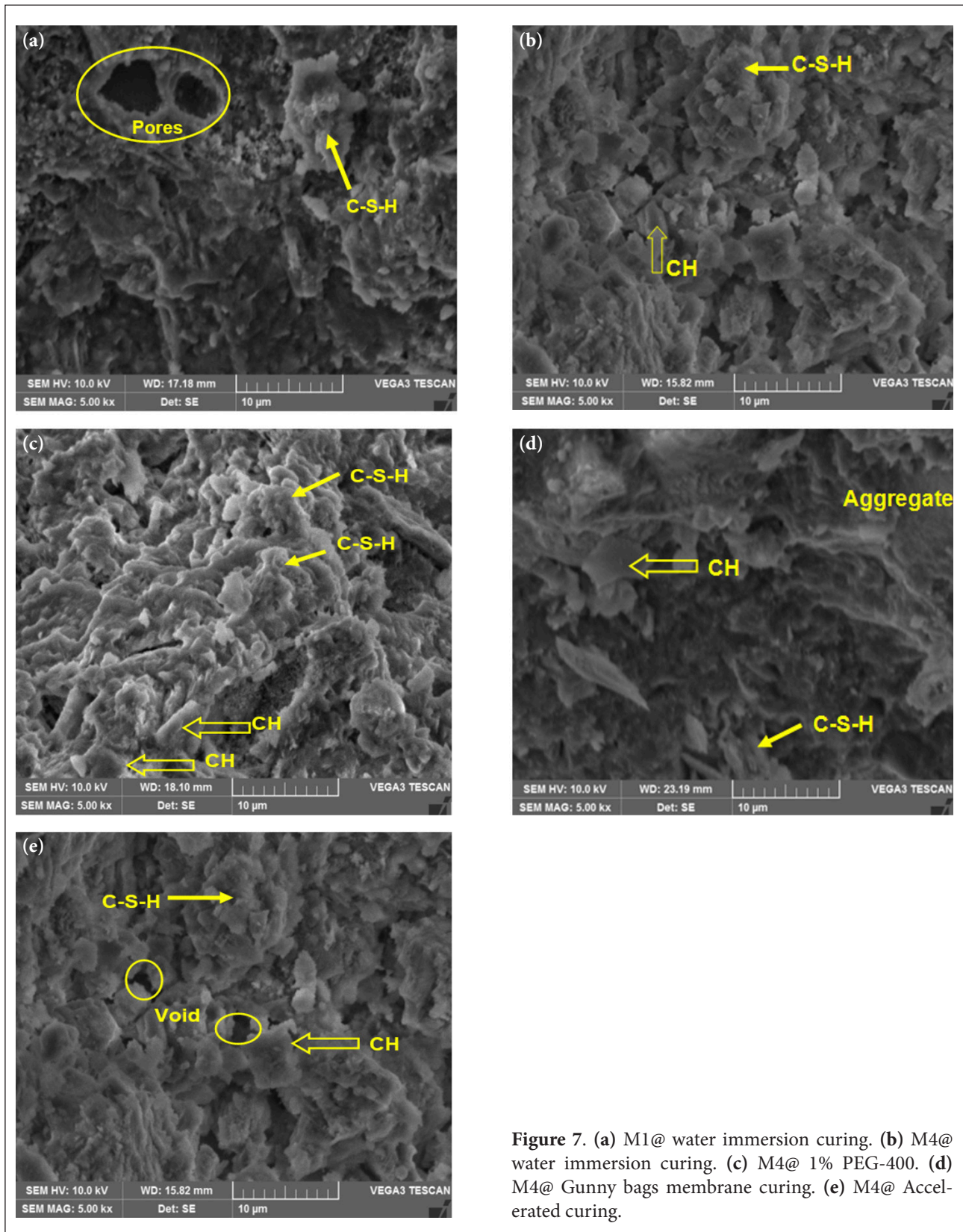
Figure 7. **(a)** M1@ water immersion curing. **(b)** M4@ water immersion curing. **(c)** M4@ 1% PEG-400. **(d)** M4@ Gunny bags membrane curing. **(e)** M4@ Accelerated curing.

3.3.2. Rapid Chloride Permeability Test

The rapid chloride permeability classification results in Figure 6 further demonstrate the reduced chloride penetrability with mineral admixtures and adequate external curing. Mix M1 had the highest permeability in the 'High' category under gunny bag curing, while metakaolin blends M5 achieved the 'Very Low' classification under water curing due to its low migration coefficient. The results indicate appropriate mix design and adequate external curing are essential to limiting chloride transport and achieving durable SCC.

Table 9. Elemental composition of optimum mixes

Mix designation	M1@WIC	M4@ WIC	M4@ 1% PEG-400	M4@ GBC	M4@ AC
Ca/Si	1.75	1.25	1.22	1.34	1.38

3.4. Scanning Electronic Microscope Analysis

The microstructure of selected optimized SCC mixes under different curing conditions was examined using scanning electron microscopy (SEM). The SEM images in Figure 7 show the morphology and hydration phases. In the plain cement mix, M1 cured by water immersion (Fig. 7a), abundant hydration products in the form of calcium silicate hydrate (C-S-H) gel and $Ca(OH)_2$ crystals can be observed filling voids and spaces between particles. The mix containing fly ash, silica fume, and metakaolin (M4) cured by water immersion (Fig. 7b) displays a denser microstructure with fewer voids owing to enhanced pozzolanic reactions and the filler effects of the mineral admixtures.

M4 cured with 1% polyethylene glycol (Fig. 7c) exhibits a reasonably dense structure, but some microcracks are visible, likely due to restrained shrinkage and moisture loss. In contrast, due to insufficient hydration and carbonation, the sample cured with gunny bags (Fig. 7d) shows a more porous structure with channels and cavities. M4 cured using accelerated techniques (Fig. 7e) displays some heterogeneity in the microstructure with regions of discontinuous hydration products.

The Ca/Si ratios in Table 9 indicate the C-S-H composition and hydration extent. The plain cement mix M1 had the highest Ca/Si ratio of 1.75 underwater curing due to $Ca(OH)_2$ and C-S-H formation. The blended mix M4 showed lower Ca/Si ratios between 1.22–1.38 owing to the pozzolanic consumption of $Ca(OH)_2$ and additional C-S-H from the reactions between silicates and the cement. Among curing regimes for M4, water immersion resulted in the lowest ratio of 1.25, suggesting the greatest hydration. The microstructural evidence correlates well with the improved mechanical and durability performance observed for the optimized metakaolin SCC blend under water curing.

4. CONCLUSION

This study demonstrated that incorporating fly ash, silica fume, and metakaolin as partial cement replacements in self-compacting concrete (SCC) improved rheological properties like flowability, passing ability, and filling ability. Metakaolin resulted in slightly higher viscosity and lower slump flow than other mixes, likely due to its finer particles and high reactivity requiring more water. However, all designed mixes satisfied EFNARC guidelines for SCC workability.

The compressive strength and chloride penetration resistance of SCC were enhanced by using mineral admixtures as cement replacements compared to plain cement mixes. Metakaolin at 20% replacement showed the best performance, increasing 28-day strength by up to 53% and reducing the chloride migration coefficient by up to 40% compared to the control. This is attributed to metakaolin's high pozzolanic reactivity, leading to refined pores and enhanced formation of secondary C-S-H.

Water immersion curing was the most effective method for curing SCC, improving 28-day compressive strength by 3–15% and reducing the chloride migration coefficient by up to 30% compared to other curing techniques. Wet curing provides an optimal hydration environment, allowing pozzolanic reactions to progress and increasing densification.

Mineral admixtures reduced the sensitivity of SCC to external curing conditions due to their ability to promote internal curing through ongoing pozzolanic reactions. Metakaolin SCC showed the least property variations between curing regimes due to its high reactivity.

Microstructural analysis revealed that mineral admixtures improved the interfacial transition zone in SCC by increasing particle packing density and enabling pozzolanic products like additional C-S-H to fill voids. Water curing produced the most refined pore structure with continuous hydration products.

ETHICS

There are no ethical issues with the publication of this manuscript.

DATA AVAILABILITY STATEMENT

The authors confirm that the data that supports the findings of this study are available within the article. Raw data that support the finding of this study are available from the corresponding author, upon reasonable request.

CONFLICT OF INTEREST

The authors declare that they have no conflict of interest.

FINANCIAL DISCLOSURE

The authors declared that this study has received no financial support.

PEER-REVIEW

Externally peer-reviewed.

REFERENCES

[1] de Souza, A. M., de Carvalho, J. M. F., Santos, C. F. R., Ferreira, F. A., Pedroti, L. G., & Peixoto, R. A. F. (2022). An analytical review of the strategies to improve the eco-efficiency of self-compacting concrete using industrial waste. *Constr Build Mater, 347*, 128634. [CrossRef]

[2] Faraj, R. H., Mohammed, A. A., & Omer, K. M. (2022). Self-compacting concrete composites modified with nanoparticles: A comprehensive review, analysis, and modeling. *J Build Eng, 50*, 104170. [CrossRef]

[3] Gupta, N., Siddique, R., & Belarbi, R. (2021). Sustainable and greener self-compacting concrete incorporating industrial by-products: A review. *J Clean Prod, 284*, 124803. [CrossRef]

[4] Dey, S., Kumar, V. P., Goud, K. R., & Basha, S. K. J. (2021). State of art review on self-compacting concrete using mineral admixtures. *J Build Pathol Rehabil, 6*(1), 18. [CrossRef]

[5] Madhavi, C., Reddy, V. S., Rao, M. S., Shrihari, S., Kadhim, S. I., & Sharma, S. (2023). The effect of elevated temperature on self-compacting concrete: Physical and mechanical properties. *E3S Web Conf, 391*, 01212. [CrossRef]

[6] Rao, T. V., Seshagiri Rao, M. V., & Rao, P. J. (2021, March 1). Strength properties of double blend and triple blend self-compacting concrete subjected to different curing methods. *IOP Conf Ser Mater Sci Eng, 1126*(1), 012085. [CrossRef]

[7] Klemczak, B., Gołaszewski, J., Smolana, A., Gołaszewska, M., & Cygan, G. (2023). Shrinkage behaviour of self-compacting concrete with a high volume of fly ash and slag experimental tests and analytical assessment. *Constr Build Mater, 400*, 132608. [CrossRef]

[8] Rao, M. D., Dey, S., & Rao, B. P. (2023). Characterization of fiber reinforced self-compacting concrete by fly ash and cement. *Chem Inorg Mater, 1*, 100010. [CrossRef]

[9] Karthiga, N., Siddharth, M. A., Kannan, V., & Dhanusree, C. (2023). Experimental investigation of self-compacting concrete (SCC) using fly ash. *Mater Today Proc, 2023*, 2023.04.582

[10] Luo, Y., Zhang, Q., Wang, D., Yang, L., Gao, X., Liu, Y., & Xue, G. (2023). Mechanical and microstructural properties of MK-FA-GGBFS-based self-compacting geopolymer concrete composites. *J Build Eng, 77*, 107452. [CrossRef]

[11] Singh, A., Mehta, P. K., & Kumar, R. (2022). Performance of binary admixtures (Fly ash and Silica fume) on self-compacting concrete. *Mater Today Proc, 58*, 970–977. [CrossRef]

[12] Jameel, G. S., İpek, S., Ahmed, A. D., Güneyisi, E., & Güneyisi, E. M. (2023). Rheological behavior and key properties of metakaolin and nano-SiO_2 blended fibrous self-compacting concretes. *Constr Build Mater, 368*, 130372. [CrossRef]

[13] Rojo-López, G., González-Fonteboa, B., Martínez-Abella, F., & González-Taboada, I. (2022). Rheology, durability, and mechanical performance of sustainable self-compacting concrete with metakaolin and limestone filler. *Case Stud Constr Mater, 17*, e01143. [CrossRef]

[14] Suprakash, A. S., Karthiyaini, S., & Shanmugasundaram, M. (2021). Future and scope for development of calcium and silica rich supplementary blends on properties of self-compacting concrete - a comparative review. *J Mater Res Technol, 15*, 5662–5681. [CrossRef]

[15] Devi, K., Aggarwal, P., & Saini, B. (2020). Admixtures used in self-compacting concrete: A review. *Iran J Sci Technol Trans Civ Eng, 44*, 377–403. [CrossRef]

[16] Frhaan, W. K. M., Bakar, H. B. A., Hilal, N., & Al-Hadithi, A. I. (2020). Effect of silica fume and super-plasticizer on mechanical properties of self-compacting concrete: A review. IOP Conf Ser Mater Sci Eng, 978(1), 012052. [CrossRef]

[17] Albiajawi, M. I., EMBONG, R., & Muthusamy, K. (2021). Influence of mineral admixtures on the properties of self-compacting concrete: An overview. *Constr, 1*(2), 62–75. [CrossRef]

[18] Danish, P., & Ganesh, G. M. (2021). Study on influence of metakaolin and waste marble powder on self-compacting concrete – a state of the art review. *Mater Today Proc, 44*, 1428–1436. [CrossRef]

[19] Venkatesh, C., Nerella, R., & Chand, M. S. R. (2020). Experimental investigation of strength, durability, and microstructure of red-mud concrete. *J Korean Ceram Soc, 57*(2), 167–174. [CrossRef]

[20] Ramkumar, K. B., Rajkumar, P. K., Ahmmad, S. N., & Jegan, M. (2020). A review on performance of self-compacting concrete – use of mineral admixtures and steel fibres with artificial neural network application. *Constr Build Mater, 261*, 120215. [CrossRef]

[21] Kumar, K. R., Shyamala, G., Awoyera, P. O., Vedhasakthi, K., & Olalusi, O. B. (2021). Cleaner production of self-compacting concrete with selected industrial rejects-an overview. *Silicon, 13*, 2809–2820. [CrossRef]

[22] Massana, J., Reyes, E., Bernal, J., León, N., & Sánchez-Espinosa, E. (2018). Influence of nano-and micro-silica additions on the durability of a high-performance self-compacting concrete. *Constr Build Mater, 165*, 93–103. [CrossRef]

[23] Güneyisi, E., Gesoğlu, M., & Algin, Z. (2013). Performance of self-compacting concrete (SCC) with high-volume supplementary cementitious materials (SCMs). *Eco-Eff Concr, 2023*, 198–217. [CrossRef]

[24] Devadass, T. (2019). Experimental study on replacement of fine aggregate in concrete with dissimilar curing conditions. *Case Stud Constr Mater, 11*, e00245. [CrossRef]

[25] Wang, Y., Wang, S., Wang, T., Song, T., Wu, X., Guo, L., Xie, W., Qiu, P., Dong, Q., & Li, Q. (2023). A green nanocomposite membrane for concrete moisturizing, with excellent barrier properties and aging resistance. *Mater Today Commun, 35*, 105553. [CrossRef]

[26] Saravanakumar, R., Elango, K. S., Piradheep, G., Rasswanth, S., & Siva, C. (2023). Effect of super absorbent polymers in properties of self-curing concrete - a state of art of review. *Mater Today Proc, 2023*, 05.117. [CrossRef]

[27] Hamada, H., Alattar, A., Tayeh, B., Yahaya, F., & Almeshal, I. (2022). Influence of different curing methods on the compressive strength of ultra-high-performance concrete: A comprehensive review. *Case Stud Constr Mater, 17*, e01390. [CrossRef]

[28] Athira, V. S., Bahurudeen, A., Saljas, M., & Jayachandran, K. (2021). Influence of different curing methods on mechanical and durability properties of alkali activated binders. *Constr Build Mater, 299*, 123963. [CrossRef]

[29] Ekolu, S. O. (2016). A review on effects of curing, sheltering, and CO_2 concentration upon natural carbonation of concrete. *Constr Build Mater, 127*, 306–320. [CrossRef]

[30] Sri Rama Chand, M., Rathish Kumar, P., Swamy Naga Ratna Giri, P., & Rajesh Kumar, G. (2018). Performance and microstructure characteristics of self-curing self-compacting concrete. *Adv Cem Res, 30*(10), 451–468. [CrossRef]

[31] ASTM C150/C150M-16e1. (2016). *Standard specification for Portland cement.* ASTM International, West Conshohocken, PA.

[32] BIS, IS 383-2016. (2016). *Specification for coarse and fine aggregates from natural sources for concrete.* Bureau of Indian Standards, New Delhi.

[33] BIS, IS 10262-2019 (2019) *Specification for concrete mix proportioning.* Bureau of Indian Standards, New Delhi.

[34] EFNARC. (2002). *Specification and guidelines for self-compacting concrete.* European Federation of Specialist Construction Chemicals and Concrete Systems, Syderstone, Norfolk, UK.

[35] ASTM C192/C192M-15. (2016). *Standard practice for making and curing concrete test specimens in the laboratory.* ASTM International, West Conshohocken, PA.

[36] ASTM C684-99. (2017). *Standard test method for making, accelerated curing, and testing concrete compression test specimens.* ASTM International, West Conshohocken, PA.

[37] IRC 15-2017. (2017). *Specification for gunny bag membrane curing for concrete pavement.* Bureau of Indian Standards, New Delhi.

[38] Madduru, S. R. C., Pancharathi, R. K., Giri, P. S. N. R., Kumar, G. R. (2018). Performance and microstructure characteristics of self-curing self-compacting concrete. *Adv Cem Res, 30*(10), 451–468. [CrossRef]

[39] BIS, IS 516: 1959. (1959). *Specification for determining compressive strength of concrete.* Bureau of Indian Standards, New Delhi.

[40] ASTM C 1202. (2012). *Standard test method for electrical indication of concrete's ability to resist chloride ion penetration.* ASTM International, West Conshohocken, PA.

[41] NT BUILD 492. (1999). *Concrete, mortar and cement-based repair materials: Chloride migration coefficient from non-steady-state migration experiments.* Nordtest, Finland.

[42] Chava, V., & Chereddy, S. S. D. (2023). Effect of calcination on the physical, chemical, morphological, and cementitious properties of red mud. *J Sustain Constr Mater Technol, 8*(4), 297–306. [CrossRef]

[43] Bellum, R. R., Al Khazaleh, M., Pilla, R. K., Choudhary, S., & Venkatesh, C. (2022). Effect of slag on strength, durability and microstructural characteristics of fly ash-based geopolymer concrete. *J Build Pathol Rehabil, 7*(1), 25. [CrossRef]

[44] Bellum, R. R., Venkatesh, C., & Madduru, S. R. C. (2021). Influence of red mud on performance enhancement of fly ash-based geopolymer concrete. *Innov Infrastruct Solut, 6*(4), 215. [CrossRef]

[45] Mukkala, P., Venkatesh, C., & Habibunnisa, S. (2022). Evaluation of mix ratios of light weight concrete using geopolymer as binder. *Mater Today Proc, 52*, 2053–2056. [CrossRef]

[46] Ruben, N., Venkatesh, C., Durga, C. S. S., & Chand, M. S. R. (2021). Comprehensive study on performance of glass fibers-based concrete. *Innov Infrastruct Solut, 6*(2), 112. [CrossRef]

[47] Venkatesh, C., Nerella, R., & Chand, M. S. R. (2021). Role of red mud as a cementing material in concrete: A comprehensive study on durability behavior. *Innov Infrastruct Solut, 6*(1), 13. [CrossRef]

[48] Anirudh, M., Rekha, K. S., Venkatesh, C., & Nerella, R. (2021). Characterization of red mud-based cement mortar; mechanical and microstructure studies. *Mater Today Proc, 43*, 1587-1591. [CrossRef]

[49] Rao, T. M., Mahesh, K., Venkatesh, C., Durga, C. S. S., Reddy, B. R., Tejaswi, P. S., & Charandeepneelesh, R. (2023). Influence of magnetization of water on mechanical and durability properties of fly ash concrete. *Mater Today Proc, 2023*, 194.

[50] Durga, C. S. S., Venkatesh, C., Muralidhararao, T., Bellum, R. R. (2023). Crack healing and flexural behavior of self-healing concrete influenced by different bacillus species. *Res Eng Struct Mater, 9*(4), 1477–1488. [CrossRef]

[51] Durga, C. S. S., Venkatesh, C., Muralidhararao, T., Bellum, R. R., Rao, B. N. M. (2023). Estimation of durability properties of self-healing concrete influenced by different bacillus species. *Res Eng Struct Mater, 9*(4), 1489–1505. [CrossRef]

[52] Venkatesh, C., Sri Rama Chand, M., Ruben, N., & Sonali Sri Durga, C. (2020). Strength characteristics of red mud and silica fume-based concrete. In Smart Technologies for Sustainable Development: Select Proceedings of SMTS 2019 (pp. 387-393). Springer Singapore. [CrossRef]